Journal of Applied Polymer Science

ABS Modified with Hydrogenated Polystyrene-*grafted*-Natural Rubber

Anawat Pisuttisap,[1] Napida Hinchiranan,[2] Garry L. Rempel,[3] Pattarapan Prasassarakich[2]
[1]Program in Petrochemistry and Polymer Science, Faculty of Science, Chulalongkorn University, Bangkok 10330, Thailand
[2]Department of Chemical Technology, Faculty of Science, Chulalongkorn University, Bangkok 10330, Thailand
[3]Department of Chemical Engineering, University of Waterloo, ON N2L3G1, Canada
Correspondence to: P. Prasassarakich (E-mail: ppattara@chula.ac.th)

ABSTRACT: Natural rubber (NR) latex was grafted by emulsion polymerization with styrene monomer, using cumene hydroperoxide/tetraethylene pentamene as redox initiator system. The polystyrene-grafted NR (PS-*g*-NR) was hydrogenated by diimide reduction in the latex form using hydrazine and hydrogen peroxide with boric acid as a promoter. At the optimum condition for graft copolymerization, a grafting efficiency of 81.5% was obtained. In addition, the highest hydrogenation level of 47.2% was achieved using a hydrazine:hydrogen peroxide molar ratio of 1:1.1. Hydrogenation of the PS-*g*-NR (H(PS-*g*-NR)) increased the thermal stability. Transmission electron microscopy analysis of the H(PS-*g*-NR) particles revealed a nonhydrogenated rubber core and hydrogenated outer rubber layer, in accordance with the layer model. The addition of H(PS-*g*-NR) at 10 wt % as modifier in an acrylonitrile–butadiene–styrene (ABS) copolymer increased the tensile and impact strengths and the thermal resistance of the ABS blends, and to a greater extent than that provided by blending with NR or PS-*g*-NR. © 2012 Wiley Periodicals, Inc. J. Appl. Polym. Sci. 129: 94–104, 2013

KEYWORDS: elastomers; mechanical properties; emulsion polymerization

Received 16 August 2012; accepted 6 October 2012; published online 3 November 2012
DOI: 10.1002/app.38691

INTRODUCTION

Acrylonitrile–butadiene–styrene copolymer (ABS) is synthesized via graft copolymerization of styrene (ST) and acrylonitrile monomers onto polybutadiene chains, which provides advantageous mechanical properties, such as increased toughness and a higher impact and chemical resistance. However, the monomers used in the formation of ABS thermoplastics are derived from petroleum, a nonrenewable and depleting resource with high economic and environmental costs. At present, "Green polymers," as modified natural rubber (NR) latex can be applied to partially substitute for the thermoplastics. Grafted NR (*g*-NR), synthesized by graft copolymerization of ST and methyl methacrylate (MMA) onto NR has been used as a modifier in thermoplastics,[1–3] since *g*-NR has good mechanical and dynamic properties, such as high elasticity and tear strength and a low heat storage. However, as a substitute for synthetic rubber, modified NR can only be used in small amounts and for limited applications, especially in the case of products that require a high weather resistance because NR is deteriorated by sunlight, ozone, and oxygen due to its high level of unsaturated carbon double (C=C) bonds. Chemical modification of NR is one method for overcoming these disadvantages, typically performed as graft copolymerization and/or hydrogenation, so as to improve the properties of NR. The hydrogenated *g*-NR (H(*g*-NR) may then be used as a "Green polymer" as an ABS modifier. The ABS/H(*g*-NR) blend ("Green ABS") could have a high potential as a new thermoplastic product in the plastics industry.

Hydrogenation is a useful method for polymer modification, as it reduces the amount of unsaturated C=C bonds and changes the properties of the diene polymer towards greater stability against thermal and oxidative degradation. Hydrogenation of NR can be achieved by both catalytic[4–8] and noncatalytic methods.[9–12] Noncatalytic hydrogenation of the unsaturated backbone of NR is usually carried out using diimide reduction in latex form.[10,11] The active hydrogen species, in the form of diimide (NH=NH) that is derived from the oxidation of hydrazine (N_2H_4), is capable of reducing the C=C bonds.[12]

There is a considerable amount of research that has been reported on graft copolymerization of vinyl monomers (MMA, ST, and acrylonitrile) onto NR latex.[1–3,13–18] For the graft copolymerization of a 1:1 (w/w) ratio of ST: MMA onto NR seed latex using cumene hydroperoxide (CHPO)/sodium formaldehyde sulfoxylate dihydrate/EDTA-chelated Fe^{2+} as a redox initiator,[13] the grafting efficiency (GE) was found to be dependent on the reaction temperature, initiator concentration, and monomer to rubber ratio.[13,14] It was also found that CHPO/tetraethylene pentamene (TEPA) could enhance the GE and was a

better redox initiator system for grafting MMA onto NR.[16] For the graft copolymerization of glycidyl methacrylate and ST onto NR, the *g*-NR product could be used as a compatibilizer for NR/Poly(methyl methacrylate) (PMMA) blends. The tensile fracture surface, as examined by scanning electron microscopy (SEM), showed that the *g*-NR acted as an interfacial agent providing good adhesion between the two phases of the blend.[19] Recently, a modified NR latex was prepared by graft copolymerization with MMA and then hydrogenated using OsHCl $(CO)(O_2)(PCy_3)_2$ as the catalyst, with a high hydrogenation degree (HD) of up to 99% being achieved.[20] The catalytic hydrogenation of PS-*g*-NR in the presence of OsHCl $(CO)(O_2)(PCy_3)_2$ was reported to improve the thermal stability of *g*-NR without affecting its glass transition temperature.[21]

Wideman[22] discovered that in the diimide hydrogenation of acrylonitrile–butadiene rubber (NBR) in latex form, the diimide species could be produced by the oxidation of hydrazine hydrate (N_2H_4)/hydrogen peroxide (H_2O_2), using copper ions as the catalyst without any pressure vessel, organic solvent or hydrogen gas. The mechanism of the diimide-mediated hydrogenation of NBR latex has been proposed to occur at the surface of the polymer particles.[23] For the diimide-mediated hydrogenation of the NR latex using N_2H_4/H_2O_2 and Cu^{2+} as the catalyst, it was found that a 67.8% HD was achieved within 6 h at 55°C, with a low rubber concentration, and that a high N_2H_4 concentration provided the optimum condition.[10] Recently, the preparation of hydrogenated skim NR latex (SNR) using the diimide reduction technique was reported, to increase the decomposition temperature of the hydrogenated SNR indicating that diimide hydrogenation increased the thermal stability of SNR.[11]

From previous work, *g*-NR was successfully hydrogenated in the presence of an Os complex catalyst, toluene, and H_2 with a 99% HD being achieved at high temperature and pressure.[20,21] In this study, PS-*g*-NR was first hydrogenated by diimide reduction and the effect of varying the reaction parameters on the HD of the obtained hydrogenated PS-*g*-NR (H(PS-*g*-NR)) was investigated. The mechanical properties and thermal stability of ABS/modified NR blends were also evaluated.

EXPERIMENTAL

Materials

NR latex with a 60% dry rubber content (DRC) was purchased from Thai Rubber Latex (Bangkok, Thailand). For graft copolymerization of NR, ST monomer, sodium dodecylsulfate (SDS), CHPO, and TEPA were supplied by Aldrich (St. Louis, USA). Isopropanol from Fisher Scientific (Loughborough, UK), potassium hydroxide (KOH) from Ajax Finechem (Seven Hills, Australia), methyl ethyl ketone (MEK) from QReC™ (Auckland, New Zealand) and petroleum ether from Mallinckrodt Chemicals (NJ, USA), were used as received.

For diimide hydrogenation of *g*-NR, hydrazine ($N_2H_4.H_2O$) and H_2O_2 (30% aqueous solution) were purchased from MERCK (Hohenbrunn, Germany). Boric acid (H_3BO_3) from QReC™ (Auckland, New Zealand) and silicone oil from Ajax Finechem (Seven Hills, Australia) were used as received. Formic acid (CH_2O_2) for rubber precipitation and d-chloroform ($CDCl_3$) for NMR analysis were purchased from Merck (Darmstadt, Germany). Deionized water was used in all experiments.

ABS pellets (SR 101, extrusion grade) were supplied by IRPC public company limited (Rayong, Thailand).

Preparation of PS-*g*-NR

The PS-*g*-NR latex was prepared by emulsion graft copolymerization. NR latex (50 g, 60% DRC) was charged into a 500-mL-four-necked glass reactor containing 100 mL of deionized water. The glass reactor was equipped with a stirrer, condenser, and nitrogen gas inlet. About 0.5 phr of KOH (0.5 parts per 100 parts of DRC, by weight) and 1 phr of SDS were then added. The mixture was deoxygenated by purging with nitrogen gas. Isopropanol (1.5 phr), as a stabilizer, was then added and the mixture was heated up to the desired temperature, whereupon the mixture of ST monomer and the CHPO initiator (1 phr) were added continuously for 1 h to attain swelling in the mixture, followed by addition of TEPA (1 phr to give a final CHPO:TEPA ratio of 1:1). The reaction was stirred for 8 h under a nitrogen atmosphere to complete the graft copolymerization.

The latex product was cast onto a glass plate at room temperature in an open tray and then dried in vacuum at 40°C until at a constant weight was achieved. The conversion of monomer was determined by a gravimetric method. Finally, *g*-NR was extracted in a soxhlet apparatus using petroleum ether and MEK as solvent. After each extraction, the weight difference between the initial and extracted samples obtained was used to determine the percentage of *g*-NR, free PS and the GE by eqs. (1)–(3):

$$\text{Grafted NR}(\%) = \frac{\text{weight of grafted NR}}{\text{weight of gross polymer products}} \times 100 \quad (1)$$

$$\text{Free PS}(\%) = \frac{\text{weight of free PS}}{\text{weight of gross polymer products}} \times 100 \quad (2)$$

$$\text{Grafting efficiency}(\%) = \frac{\text{weight of monomer grafted}}{\text{total weight of monomer polymerized}} \times 100 \quad (3)$$

Hydrogenation of PS-*g*-NR

The *g*-NR latex was charged into a 500-mL glass reactor. KOH (1 phr), catalyst and hydrazine were added and heated to the reaction temperature. H_2O_2 was added drop-wise over a specific period of time. If many bubbles formed during the addition of H_2O_2, a small amount of silicone oil was added to minimize foaming. After the 6 h reaction time, the latex mixture was postreacted for 30 min while cooling to room temperature.

Preparation of ABS/Modified Rubber Blends

The ABS/NR, ABS/PS-*g*-NR, and ABS/H(PS-*g*-NR) blends were prepared at various weight ratios of ABS: modified rubbers by a melt-mixing system. The ABS pellet was fed into the chamber for 3 min and then blended with the modified NR for 12 min. All samples (200 g/batch) were blended at 80 rpm (rotor speed) and the mixing-roll temperature was kept constant at 190°C. The mixed compounds were kept at room temperature for 24 h. Then, these compounds were cut into pellets by a crusher

Applied Polymer SCIENCE

machine and pressed by compression-molding at 190°C with a pressure of 120 kg/cm^2 for 13 min.

Characterization

The HD (%) of the H(PS-*g*-NR) was determined by proton nuclear magnetic resonance (^{1}H-NMR) spectroscopy using a Bruker 300 MHz spectrometer with $CDCl_3$ as the solvent, by integration of the peak area for the saturated protons (—CH_2— and —CH_3) and that of the unsaturated protons.

Thermogravimetric analysis (TGA) of the modified rubber sample was performed on a Perkin-Elmer Pyris Diamond TG/DTA and TGA thermograms were recorded at a heating rate of 10°C/min under a nitrogen environment from room temperature to 900°C. The initial decomposition temperature (T_{id}) and the temperature at the maximum mass loss rate (T_{max}) were evaluated.

The glass transition temperature (T_g) of grafted and hydrogenated samples were obtained using a Mettler Toledo DSC 822 differential scanning calorimeter (DSC). The sample, in an aluminum pan, was cooled down to −100°C with liquid nitrogen and then heated up to 40°C at a constant heating rate of 10°C/min under a nitrogen atmosphere. The midpoint of the baseline shift was taken as the T_g value.

Transmission electron microscopy (TEM) based observation of the morphology of the modified rubbers was performed using a JEOL JEM-2010 transmission electron microscope at 80 kV. A small amount of latex sample was dispersed in water and dropped on the grid. The thin sections of samples were stained with OsO_4 vapor for 24 h before observation.

The mechanical properties of the ABS blends were measured following ASTM test methods. The tensile properties of ABS/rubber blends after and before thermal aging at 165°C for 25 min were measured in terms of their tensile strength (TS) and elongation at break (E_B) according to ASTM D 638. The specimens were cut from a 3.0 mm thick sheet and the average of five specimens was considered as the representative value. The tensile test of all blend samples was conducted on a Universal testing machine (LLOYD Instrument LR 10K Plus) at a crosshead speed of at 10 mm/min.

Izod impact testing was conducted on GOTECH GT 7045 Impact tester in accordance with ASTM D256. Specimens were notched and the notched width along with the thickness of each specimen was measured before testing. The impact energy was obtained by the difference in the potential energy of the falling hammer after and before impact. Impact energy per cross-section area of specimen is expressed as the impact strength. The average impact strength was calculated for each group of specimens. The hardness was measured using a Durometer Shore-type-D machine at room temperature, where the test specimen had a minimum thickness of 6 mm, according to ASTM D 785.

The morphology of the ABS/modified rubber blends from the tensile test was observed by scanning electron microscopy (SEM) using a JEOL JSM-6400 scanning electron microscope at an accelerating voltage of 15 kV and a magnification of 5000×. All samples were fractured after immersion in liquid nitrogen for about 10 min. The fracture surface was then coated with a thin layer of gold.

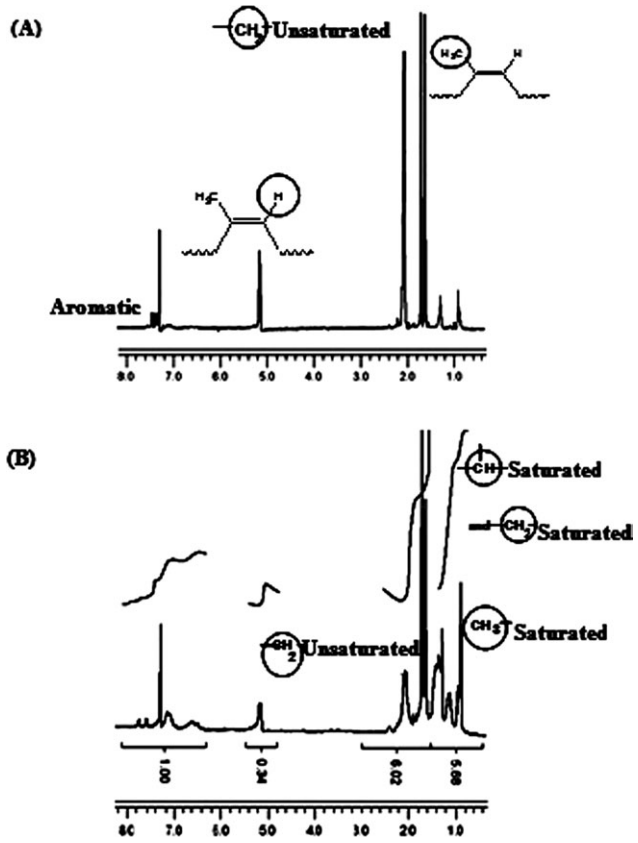

Figure 1. ^{1}H-NMR spectra of (A) PS-*g*-NR, and (B) H(PS-*g*-NR) with a 47% HD.

RESULTS AND DISCUSSION

Characterization

To determine the presence of the grafted NR, the products were extracted by petroleum ether and MEK. After solvent extraction, the graft copolymer was analyzed by ^{1}H-NMR spectroscopy. The ^{1}H-NMR spectrum of the *g*-NR revealed two major peaks at 1.64 and 2.01 ppm that are assigned to the aliphatic group (—CH_3; 1.64 ppm and —CH_2—; 2.01 ppm) of the NR, while that at 5.15 ppm peak is assigned to the *cis*-olefinic proton (—HC=CH—) in the NR [Figure 1(A)]. The signals at 6.5–7.5 ppm are attributed to the peaks of aryl protons within the PS graft chains. Thus, the ^{1}H-NMR spectrum indicated that during the emulsion polymerization the ST was grafted (as PS) onto the NR.

The ^{1}H-NMR spectrum of the hydrogenated PS-*g*-NR (HD of 47.2%) revealed two major peaks that are attributed to the aliphatic group (—CH_3; 1.64 ppm and —CH_2—; 2.01 ppm) of the NR as well as the peaks of the PS aryl protons (range of 6.5–8.0 ppm) within the PS graft [Figure 1(B)]. The signal for the *cis*-olefinic protons (—HC=CH—) were centered at 5.15 ppm. When the HD increased, the intensity of the *cis*-olefinic proton peaks decreased and new peaks appeared at 0.8–1.8 ppm that

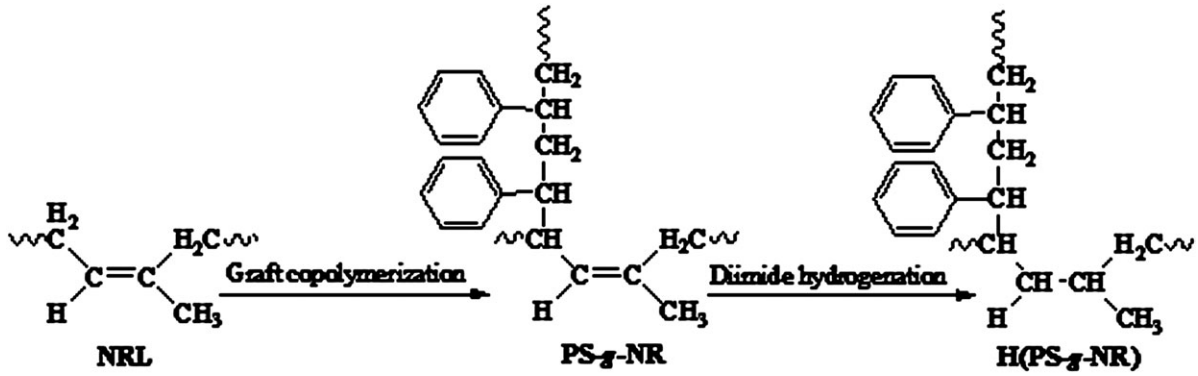

Scheme 1. Structures of PS-*g*-NR and H(PS-*g*-NR).

were attributed to the —CH_3 and saturated —CH_2— units. Graft copolymerization and hydrogenation were confirmed by the structure of H(PS-*g*-NR), and are shown in Scheme 1.

Graft Copolymerization of ST onto NR Latex to Form PS-*g*-NR

The results of graft copolymerization of ST onto NR latex (to form PS-*g*-NR) using emulsion polymerization are summarized in Table I. The PS-*g*-NR products consisted of 69.0–82.3% *g*-NR, 8.8–24.3% free NR and 6.6–16.6% free PS, depending on the temperature and the DRC, with a ST conversion and GE of 36.5–61.7% and 56.4–81.5%, respectively.

The effect of varying the DRC concentration on the monomer conversion and grafting properties was studied at 10–30% DRC at a reaction temperature of 50 or 60°C. The reactions were performed with an initiator concentration of 1 phr, ST: rubber ratio of 1 and a reaction time of 8 h in all cases. The degree of monomer conversion decreased with a decreasing DRC (or increasing water content), which could be explained by the transfer of ST through the larger aqueous phase resulting from the addition of water. The grafting was diffusion controlled due to the fact that the ST diffused from the monomer droplets to the surface of NR particles through the large aqueous phase.

The effect of the reaction temperature on the monomer conversion and grafting properties was studied at 50 and 60°C. With respect to grafting ST onto NR, increasing the reaction temperature from 50 to 60°C did not significantly affect the monomer conversion % and *g*-NR levels however the GE at higher DRC levels decreased (Table I). The GE obtained during the graft copolymerization of MMA and ST onto NR was reported to decrease at temperatures above 60°C, because a large amount of the free radicals produced at the higher temperature combine with themselves.[13]

Hydrogenation of PS-*g*-NR

In this study, the *g*-NR latex with 73.0% grafted NR, 10.4% free NR, 16.6% free PS, and a 56.4%GE (PS-*g*-NR_10 in Table I) was selected to be used as the substrate material for subsequent diimide hydrogenation. The effect of the concentration of hydrazine, H_2O_2, and H_3BO_3 on the HD of the obtained H(PS-*g*-NR) are summarized in Table II.

H_3BO_3 is an alternative material used to help promote diimide hydrogenation due to its unique ability to provide a higher and a more stable rate for the diimide reaction.[24,25] It has been suggested that H_3BO_3 lowers and mediates the concentration of H_2O_2 via the formation of hydrogen-bonds that stabilize the H_2O_2 and so reduces its oxidative activity.

Table I. Effect of the Dry Rubber Content (DRC) and Reaction Temperature on the Graft Copolymerization of Styrene Monomers (ST) onto Natural Rubber Latex (NR) in Terms of the % Conversion (Conv.) and Grafting Efficiency (GE)

					Grafting properties			
Exp.	Wt of NR (g)	Temp (°C)	DRC (%)	Conv (%)[1]	*g*-NR (%)	Free NR (%)	Free PS (%)	GE (%)
PS-*g*-NR_1	50	50	10	37.9	81.5	11.4	7.2	73.9
PS-*g*-NR_2	50	50	15	42.1	81.7	11.4	6.8	76.9
PS-*g*-NR_3	50	50	20	54.7	74.0	19.5	6.6	81.5
PS-*g*-NR_4	50	50	30	53.0	69.0	24.3	6.8	80.5
PS-*g*-NR_5	50	60	10	40.0	79.1	13.2	7.7	72.9
PS-*g*-NR_6	50	60	15	43.9	79.1	13.6	7.4	75.8
PS-*g*-NR_7	50	60	20	36.5	82.3	11.1	6.6	75.5
PS-*g*-NR_8	50	60	30	50.7	74.2	14.1	11.7	65.3
PS-*g*-NR_9	100	50	30	50.4	76.9	8.8	14.4	57.1
PS-*g*-NR_10	100	60	30	61.7	73.0	10.4	16.6	56.4

Condition: Initiator = 2 phr, monomer-to-rubber ratio = 1:1, time = 8 h.

Table II. Effect of Process Parameters on the Hydrogenation Degree (HD) of H(PS-*g*-NR)

Exp.	H_3BO_3 (mM)	N_2H_4 (M)	H_2O_2 (M)	$[N_2H_4]$: $[H_2O_2]$	HD (%)
1	38.8	2.33	5.27	1: 2.3	40.5
2	74.7	2.33	5.27	1: 2.3	44.1
3	116.7	2.33	5.27	1: 2.3	37.0
4	155.3	2.33	5.27	1: 2.3	34.5
5	74.7	1.27	5.27	1: 4.2	31.8
6	74.7	4.73	5.27	1: 1.1	47.2
7	74.7	6.60	5.27	1: 0.8	41.3
8	74.7	2.33	2.60	1: 1.1	36.2
9	74.7	2.33	6.60	1: 2.8	43.6
10	74.7	2.33	7.93	1: 3.4	38.9

Condition: Total volume = 150 mL, [C=C] = 0.55 M, temp = 70°C, time = 6 h.

The effect of the H_3BO_3 catalyst concentration was studied over the range of 38.8–155.3 m*M* (Exp. 1–4 in Table II), with the hydrogenation reaction performed at 70°C for 6 h. The concentration of C=C (0.55*M*), N_2H_4 (2.33*M*), and H_2O_2 (5.27*M*) were kept constant. The HD increased when the concentration of H_3BO_3 was increased from 38.8 to 74.7 m*M*, but thereafter decreased with a further increase in the H_3BO_3 concentration. The initial increase in the hydrogenation level can be explained by the formation of H-bonds between H_3BO_3 and H_2O_2 which retards the side reaction of H_2O_2 and accelerates the H_2O_2 dissociation to generate a higher concentration of the diimide radical species. On the other hand, at higher concentrations of

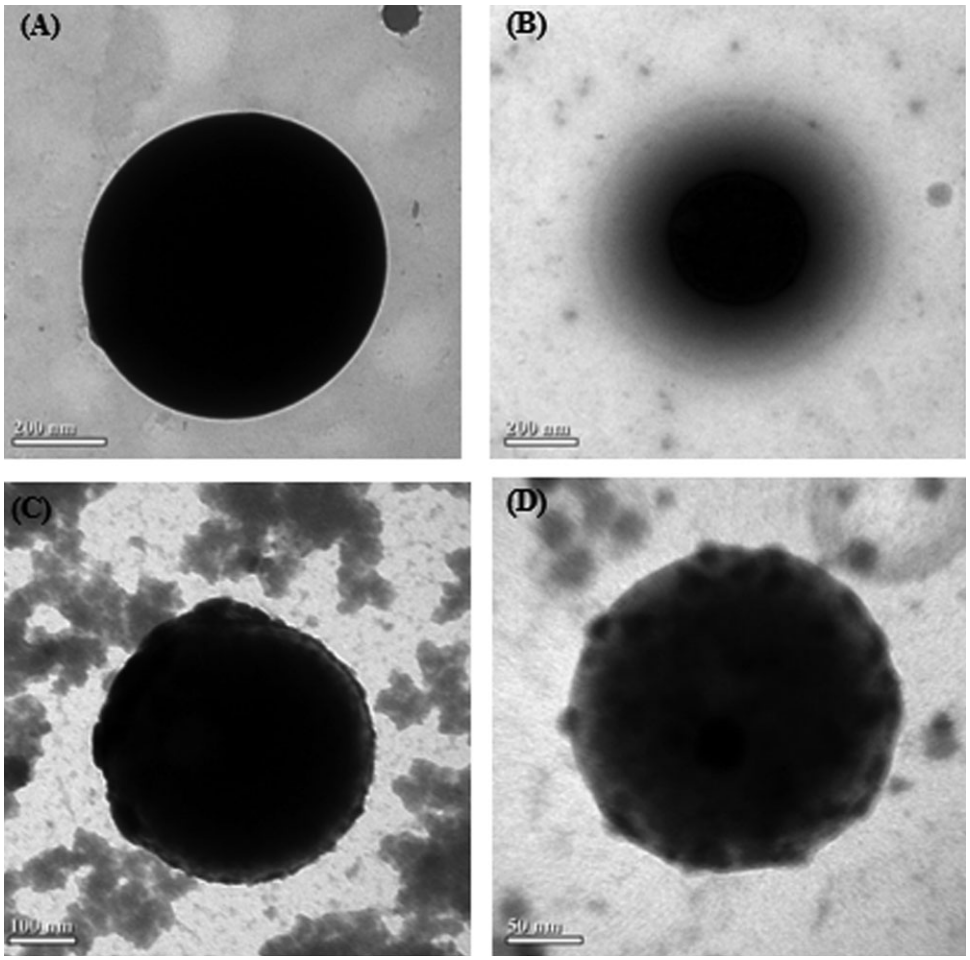

Figure 2. TEM micrographs of (A) NR, (B) PS-*g*-NR, and (C, D) H(PS-*g*-NR) at a HD of (C) 34.5% or (D) 47.2%.

H_3BO_3 (above 74.7 m*M*), free H_3BO_3 is present in the water. The N_2H_4 decomposition mostly occurs in the aqueous phase resulting in a reduction of the diimide molecules, according to eqs. (5) and (6), and a decrease in the HD.[26] The disproportionation/decomposition reactions can be represented as shown in eqs. (4) and (5), respectively:

$$HN{=}NH \rightarrow N_2 + H_2 \quad (4)$$

$$2HN{=}NH \rightarrow NH_2{-}NH_2 + N_2 \quad (5)$$

The effect of varying the hydrazine concentration on diimide hydrogenation was studied over the range of 1.27–6.60 M (Exp. 2, 5–7 in Table II), whilst maintaining the concentration of C=C (0.55*M*), H_3BO_3 (74.7 m*M*), and H_2O_2 (5.27*M*) constant. The HD increased with increasing N_2H_4 concentration up to 4.73*M*, (N_2H_4:H_2O_2 molar ratio of 1:1.1), but then decreased with a further increase in the N_2H_4 concentration to 6.60*M* (Table II). In the former case, it is likely that more diimide was produced and enhanced the N_2H_2/C=C reduction. To explain this result, the possible reactions between hydrazine and hydrogen peroxide are as shown in eqs. (6)–(8):

$$NH_2{-}NH_2 + H_2O_2 \rightarrow NH{=}NH + 2H_2O \quad (6)$$

$$NH{=}NH + {-}CH{=}CH{-} \rightarrow N_2 + {-}CH_2{-}CH_2{-} \quad (7)$$

$$NH_2{-}NH_2 + 2H_2O_2 \rightarrow N_2 + 4H_2O \quad (8)$$

Diimide molecules are produced by the reaction between N_2H_4 and H_2O_2 [eq. (6)]. In the NR latex medium which includes the C=C unsaturated unit, with H_3BO_3 as the prompter, the diimide species reacted with C=C to increase the HD [eq. (7)], and decrease the residual C=C bond level, which in the presence of an excess level of H_2O_2 leads to the conversion of N_2H_4 to N_2 [eq. (8)] and not further C=C bond reduction. Thus, the increase in the N_2H_4 concentration from 1.27*M* to 4.73*M* leads to more diimide being produced and enhanced the N_2H_2/C=C reduction resulting in an increase in the HD. As the concentration of N_2H_4 increased above 4.73 M the HD is decreased since the diimide species can self-react at higher concentrations and thus decrease the hydrogenation efficiency [eqs. (5)–(8)]. Alternatively, the excess content of diimide in this system may be dispersed into the aqueous phase.[26] A similar result was also reported by Mahittikul et al.[10]

Finally, the amount of H_2O_2 was varied over the range of 2.60–7.93*M* (Exp. 2, 8–10; Table II), while the concentration of C=C (0.55*M*), N_2H_4 (2.33*M*), and H_3BO_3 (74.7 m*M*) were kept constant. The HD initially increased with an increase in the concentration of H_2O_2 from 2.60 up to 6.60*M*, but then decreased slightly at the higher H_2O_2 concentration of 7.93*M*. This phenomenon may be explained from the two competitive reactions between N_2H_4 and H_2O_2 [eqs. (5) and (8)]. At high H_2O_2 concentrations, the decrease in HD probably is due to the fact that more H_2O_2 resided mostly in the aqueous phase and must penetrate through the NR phase at a higher rate than the rate of reaction, eq. (8). The HD may depend upon the competition between reactions, eqs. (6) and (8). At lower H_2O_2 concentrations, the diimide has more chance to diffuse into the rubber phase and so a higher HD was achieved.[27] On the basis of the reaction stoichiometry to produce diimide molecules [eq. (6)], the suitable N_2H_4:H_2O_2 molar ratio for the generation of the diimide species would be 1:1 and not the observed 1:1.1. The slight discrepancy between the theoretical and empirical optimal ratio could result from the decomposition of H_2O_2, where an apparent excess of H_2O_2 is required to compensate for this and thus maintain the effective production of diimide. Nevertheless, the highest HD was obtained with 74.7 m*M* H_3BO_3, 4.73*M* N_2H_4, 5.27*M* H_2O_2 (1:1.1 molar ratio of N_2H_4:H_2O_2), at 70°C for 6 h using a C=C ratio of 0.55*M* in a reaction volume of 150 mL.

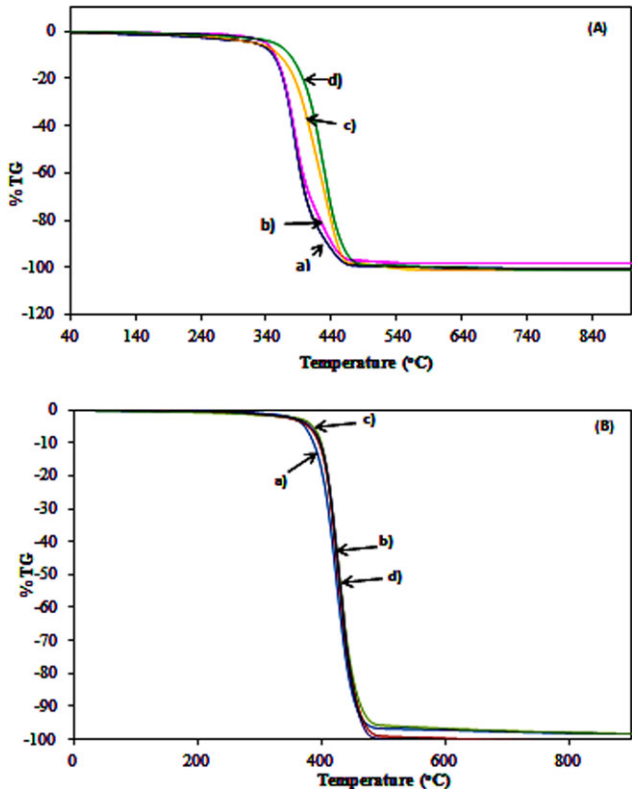

Figure 3. TGA thermograms of (A) the pure and modified rubber, as (a) NR, (b) PS-*g*-NR, and (c,d) H(PS-*g*-NR) at a HD of (c) 35.6% and (d) 47.2%; and (B) the ABS/H(PS-*g*-NR) blends at (a) 0, (b) 5, (c) 10, and (d) 20% (w/w) H(PS-*g*-NR). [Color figure can be viewed in the online issue, which is available at wileyonlinelibrary.com.]

Morphology of the Modified NR

The morphology of the NR latex and PS-*g*-NR particles, as evaluated by TEM, was of a spherical shape having a smooth surface (Figure 2). The surface morphology of the PS-*g*-NR particles was further observed by OsO_4 staining of the NR C=C bonds to increase the contrast and gradation of the particles. The darker area represents the NR core region, whereas the lighter area represents the PS grafted onto the NR as a shell [Figure 2(B)]. Thus, PS-*g*-NR particles showed a core-shell morphology with NR as the core and graft PS as the shell.

The morphology the H(PS-*g*-NR) particles with a HD of 34.5% and 47.2% also showed the core region of NR and PS grafted shell

Table III. Glass Transition (T_g), Initial Decomposition Temperature (T_{id}) and Temperature at the Maximum Mass Loss (T_{max}) of the NR and Modified NRs as well as the ABS/Modified NR Composite Blends

Rubber	HD (%)	Blend ratio (ABS/rubber)	T_g (°C)	T_{id} (°C)	T_{max} (°C)
NR	-	-	−66.6	358.0	386.2
PS-*g*-NR	-	-	−65.1, 96.2[a]	360.4	389.3
H(PS-*g*-NR)	35.6	-	−65.3, 95.2[a]	373.9	415.4
	37.8	-	−64.5, 94.6[a]	382.9	421.2
	41.3	-	−64.9, 93.4[a]	385.4	422.0
	47.2	-	−64.7, 92.9[a]	394.2	422.9
ABS	-	100/0	100.5	395.0	422.0
ABS/NR	-	95/5	100.8	395.4	424.1
	-	90/10	101.7	394.6	424.6
	-	80/20	101.9	385.9	421.3
ABS/PS-*g*-NR	-	95/5	101.1	400.6	427.5
	-	90/10	100.7	398.3	426.7
	-	80/20	101.7	394.1	424.9
ABS/H(PS-*g*-NR)	-	95/5	100.4	402.4	427.3
	-	90/10	99.8	403.0	428.9
	-	80/20	101.4	405.1	429.0

[a] T_g values are shown as those for (NR, PS).

[Figure 2(C,D)]. For the H(PS-*g*-NR) particles with a 34.5% HD, there was a very slight contrast between the core and the thin hydrogenated layer, whereas with a 47.2% HD, the contrast between the core and much lighter color shell was more clearly observed due to the lower level of residual C=C bonds stained with the OsO_4. The formation of the H(PS-*g*-NR) particles, therefore, seemed to be hydrogenated from the outer surface layer to the center of the rubber particle, in accord with a layer model.[10]

Thermal Properties of ABS/Modified NR Blends

The TGA thermograms for the NR, PS-*g*-NR, and H(PS-*g*-NR) rubbers indicate that decomposition is an overall one-step reaction because the decomposition curve of the sample occurs in one-step and provides a smooth weight loss curve [Figure 3(A)]. The glass transition temperature (T_g), the initial decomposition temperature (T_{id}) and maximum decomposition temperature (T_{max}) of the NR, PS-*g*-NR, and the H(PS-*g*-NR) of different HD, as evaluated from the TGA analysis, are summarized in Table III. The T_{id} and T_{max} of H(PS-*g*-NR) sample increased with decreasing levels of C=C bonds (increasing HD), and at each hydrogenation level were higher than that of the NR (ΔT_{id} = 15.9–36.2°C and ΔT_{max} = 29.2–36.7°C) and PS-*g*-NR (ΔT_{id} = 13.5–33.8°C and ΔT_{max} = 26.1–33.6°C). Therefore, hydrogenation (reduction of the C=C level) improves the thermal stability of the PS-*g*-NR. The DSC thermograms of H(PS-*g*-NR) indicated a two-step base-line shift, in which the lower T_g is that of NR and the upper T_g is that of PS (Figure 4). The derived T_g values for NR and PS in each of the NR, PS-*g*-NR, and H(PS-*g*-NR) (at various hydrogenation levels) are presented in Table III. The T_g of H(PS-*g*-NR) samples showed a slight reduction with increasing HD.

With respect to the ABS/modified rubber blends, the TGA thermograms of the ABS blends also revealed an overall one-step decomposition process with a smooth weight loss curve [Figure 3(B)]. The T_{id} and T_{max} values of the ABS/H(PS-*g*-NR) blends slightly increased with increasing contents of the H(PS-*g*-NR), and were higher than that of the ABS, ABS/NR, and ABS/PS-*g*-NR blends (Table III). Therefore, the addition of H(PS-*g*-NR) can improve the thermal stability of ABS. In contrast, the T_{id} and T_{max} values decreased with increasing PS-*g*-NR levels in the ABS composite rubbers. However, the T_g of the ABS/rubber blends at various rubber contents, as derived from the DSC analysis, did not significantly vary regardless of the blend composition, but rather the T_g of the ABS/NR, ABS/PS-*g*-NR, and ABS/H(PS-*g*-NR) blends remained in the range of 99.8–101.9°C (Table III). Thus, the addition of modified rubber into the ABS did not affect the resultant T_g of the ABS blends.

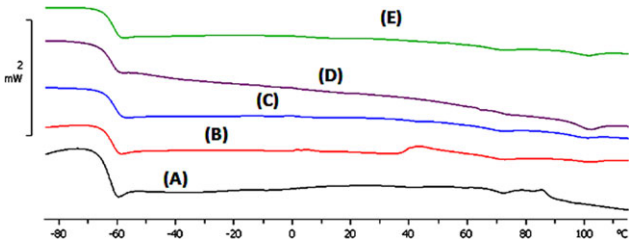

Figure 4. DSC thermograms of (A) NR, (B) H(PS-*g*-NR) 35.6% HD, (C) H(PS-*g*-NR) 37.8 % HD, (D) H(PS-*g*-NR) 41.3% HD and (E) H(PS-*g*-NR) 47.2% HD. [Color figure can be viewed in the online issue, which is available at wileyonlinelibrary.com.]

Table IV. Effect of Modified Natural Rubber Content on Mechanical Properties of ABS Blends

Compound	ABS: rubber (w/w)	TS[a] (MPa)	E_B[a] (%)	ME[a] (MPa)	IS[a] (kJ/m^2)	Hardness
ABS	100/0	34.9 (0.62)	8.79 (0.19)	538.2 (25.43)	188.2 (8.06)	71.0 (1.00)
ABS/NR	95/5	28.7 (0.36)	9.19 (0.07)	464.4 (18.16)	194.3 (1.78)	68.7 (0.58)
	90/10	24.3 (0.49)	9.53 (0.92)	415.0 (36.21)	188.4 (3.44)	67.7 (0.58)
	80/20	13.5 (0.70)	7.36 (0.35)	300.7 (27.99)	148.0 (10.15)	60.7 (0.58)
ABS/PS-*g*-NR	95/5	30.0 (0.19)	9.28 (0.40)	492.6 (8.71)	212.4 (6.68)	69.7 (0.58)
	90/10	32.0 (0.49)	9.28 (0.55)	507.2 (12.21)	261.0 (7.63)	68.0 (0.00)
	80/20	15.6 (0.18)	7.70 (0.40)	327.2 (14.50)	170.6 (7.33)	61.3 (0.58)
ABS/H(PS-*g*-NR)	95/5	34.8 (0.36)	9.44 (0.50)	553.4 (22.11)	260.7 (8.18)	70.0 (0.00)
	90/10	37.9 (0.86)	9.61 (0.26)	629.0 (18.13)	277.9 (3.93)	70.7 (0.58)
	80/20	17.5 (0.49)	8.66 (0.40)	338.4 (14.42)	178.9 (11.79)	63.7 (0.58)

[a]Mechanical properties are shown as the tensile strength (TS), elongation at break (E_B), modulus of elasticity (ME), Impact strength (IS), and hardness.

Mechanical Properties of the ABS/Modified NR Blends

The chemical modification via graft copolymerization and diimide hydrogenation changes the physical and thermal properties of the NR, and accordingly the H(PS-*g*-NR) could potentially be used as a substitute material for synthetic rubber in ABS. The H(PS-*g*-NR) (Exp. 6, Table II) and the PS-*g*-NR_10 with a GE of 56.4% were selected for blending with ABS for a comparative study. The mechanical properties of the ABS blends at various ABS to modified NR ratios are summarized in Table IV.

The tensile strength of the ABS/NR blends decreased with increasing NR levels in the blend and exhibited a significantly lower tensile strength (13.5–28.7 MPa) than that for ABS (34.9 MPa). This results from the incompatibility of NR with ABS and, especially, from the polar acrylonitrile segment and the high C=C level of NR. With respect to the ABS/PS-*g*-NR blends, the tensile strength decreased slightly with the addition of the PS-*g*-NR at 5 wt %, increased slightly at 10 wt % and then decreased significantly at 20 wt %. However, the tensile strength of the ABS/PS-*g*-NR blends at a 5–20 wt % rubber content (15.6–30.0 MPa) were all higher than that of the ABS/NR at the same proportion due to the presence of the PS component in the PS-*g*-NR. For ABS blends with various amounts of H(PS-*g*-NR), the tensile strength was unaffected by the addition of H(PS-*g*-NR) at 5 wt %, increased with a H(PS-*g*-NR) content of 10 wt % and significantly decreased at 20 wt % H(PS-*g*-NR). However, the tensile strength of the ABS/H(PS-*g*-NR) blend at a 10 wt % rubber content (37.9 MPa) was higher than that of ABS, ABS/NR, and ABS/PS-*g*-NR because of the greater chemical identical nature of the segment of graft PS chain in the NR with the graft chain in ABS and the low C=C content in the NR that increased the compatibility with ABS.

The elongation at break (E_B) of the ABS/modified rubber blends increased with increasing rubber content up to 10 wt %, but then slightly decreased at rubber contents of 20 wt % for all three types [NR, PS-*g*-NR, and H(PS-*g*-NR)]. However, although the same trend was seen, the ABS/H(PS-*g*-NR) and ABS/PS-*g*-NR blends had a higher elongation at break than ABS alone or ABS/NR blends, presumably due to the larger concentration of soft segments of NR with C=C units.[28]

The modulus of elasticity (ME) of the ABS/NR blends dramatically decreased in a dose-dependent manner with increasing NR content, which may be due to the addition of NR as a soft polymer. For the ABS/PS-*g*-NR blends, the modulus of elasticity decreased with a low PS-*g*-NR content (5 wt %), increased slightly at 10 wt %, and then significantly decreased at 20 wt %, whereas for the ABS/H(PS-*g*-NR) blends the modulus of elasticity increased at 5 and 10 wt % before being significantly reduced at 20 wt % H(PS-*g*-NR). The modulus of elasticity of the ABS/H(PS-*g*-NR) blends at a 5 and 10 wt % rubber content

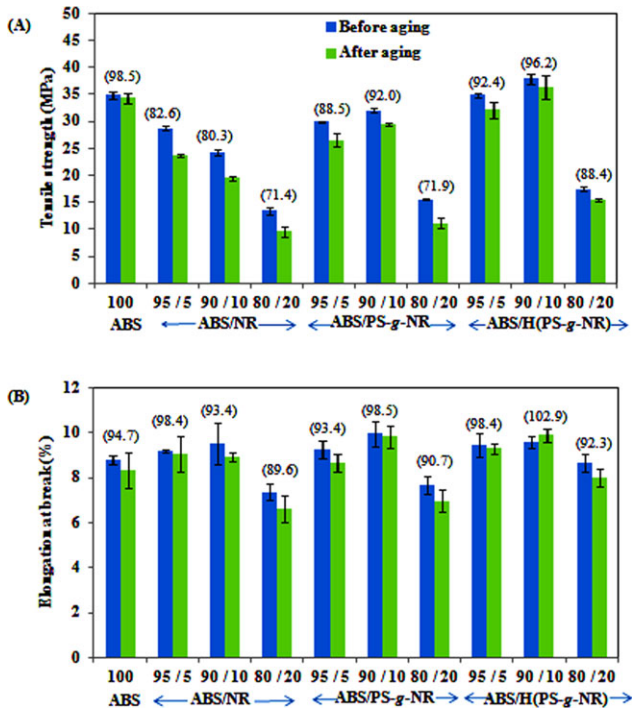

Figure 5. Effect of the modified NR content on the thermal aging (at 65°C for 25 min) of the ABS/modified NR blends on the (A) tensile strength, and (B) elongation at break, ( ) = % retention. [Color figure can be viewed in the online issue, which is available at wileyonlinelibrary.com.]

Applied Polymer SCIENCE

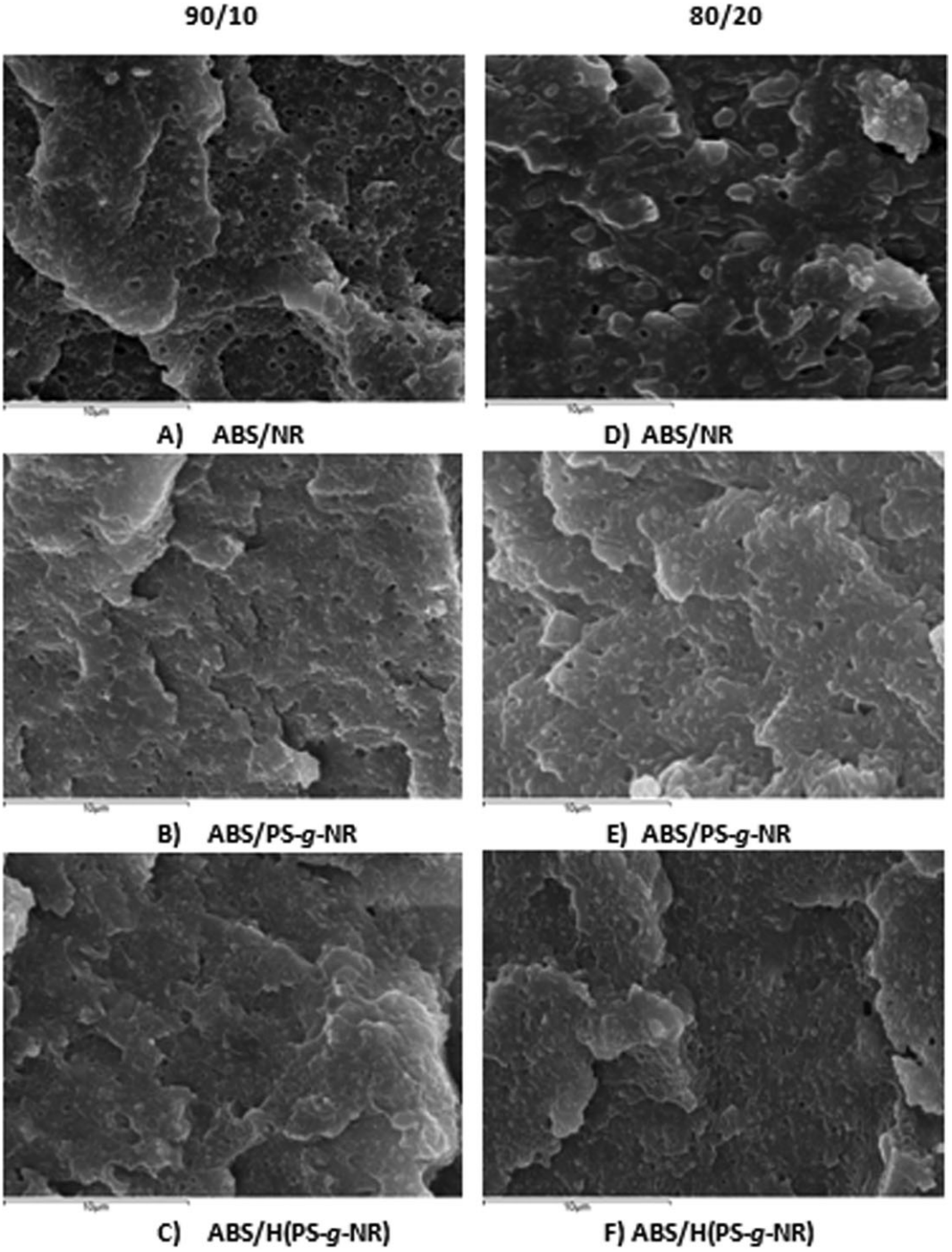

Figure 6. SEM micrographs (5000 x magnification) of ABS/modified rubber blends at (A–C) 10% (w/w) or (D–F) 20% (w/w) modified rubber, for the (A, D) ABS/NR, (B, E) ABS/PS-*g*-NR, and (C, F) ABS/H(PS-*g*-NR) blends.

were higher than that of ABS, ABS/NR and ABS/PS-*g*-NR. The increase in the modulus may be due to the rigidity of the spherical clusters of graft PS that restrict the NR main chain movement.

The hardness of the ABS/NR blends decreased with increasing NR content due to the softness of NR compared to ABS. For the ABS/PS-*g*-NR and ABS/H(PS-*g*-NR) blends, the hardness did not significantly change with the inclusion of the modified rubber at 5–10 wt %, but decreased at a modified rubber content of 20 wt %.

The impact strength (IS) of ABS was improved in all three types of blends (NR, PS-*g*-NR, and H(PS-*g*-NR)) when incorporated at 5 and 10 wt %, but the ABS blend with 10 wt % H(PS-g-NR) had the highest impact strength (277.9 kJ/m^2). This indicates that the H(PS-*g*-NR) provided a better compatibility with ABS than NR and PS-*g*-NR, presumably because of the good

miscibility of H(PS-*g*-NR) in the ABS matrix. For the ABS/NR blends, the impact strength decreased with increasing NR content (5, 10, and 20 wt %) due to their incompatibility, as observed in the SEM micrographs (Figure 6). For the ABS/PS-*g*-NR and ABS/H(PS-*g*-NR) blends, the decreased impact strength at a rubber content of 20 wt % might reflect the immiscibility and incompatibility of rubber and thermoplastics.[29]

Thermal Aging of ABS/Modified NR Blends

The thermal stability of the ABS/modified rubber blends was measured in terms of the retention (%) of their mechanical properties after thermal aging at 165°C for 25 min (Figure 5). The ABS/NR blends showed the lowest retention level of tensile strength (71.4–82.6%) and elongation at break (89.6–98.4%) after aging, while the ABS/PS-*g*-NR blends retained their tensile strength and elongation at break within 71.9–92.0% and 90.7–98.5%, respectively. However, the ABS/H(PS-*g*-NR) blends retained the highest levels of tensile strength and elongation at break, at some 88.4–96.2% and 92.3–102.9% respectively, after aging. Thus, the addition of H(PS-*g*-NR) in the ABS blend provides a greater heat resistance than the addition of NR and PS-*g*-NR, presumably due to the lower C=C level in the main chains of the NR in the H(PS-*g*-NR).

Morphology of ABS/Modified Rubber Blends

Representative SEM micrographs revealing the fracture surface of ABS/modified NR blends at various ratios are shown in Figure 6. The addition of NR to ABS at 10 wt % resulted in the NR particles forming small domains dispersed in the ABS matrix, with the NR domain sizes ranging from 1 to 10 μm [Figure 6(A)]. The interface between the two phases is very weak and the blend has many cavitations inside the ABS-whitening zone, indicating the total incompatibility of the ABS/NR polymer blend, consistent with the observed reduction in the tensile strength. For the ABS/PS-*g*-NR blends at a 10 wt % PS-*g*-NR content [Figure 6(B)], the PS-*g*-NR domains tend to connect with each other and the shape of the phase becomes regular. All the rubber particles inside the ABS-whitening zone still have cavitations but the amount of such is much lower than that in the ABS/NR blends. The ABS/H(PS-*g*-NR) blends at a 10 wt % H(PS-*g*-NR) content [Figure 6(C)] show an almost homogeneous continuous phase morphology with no or very few cavitations of rubber particles inside the ABS whitening zone, indicating a good interfacial bonding between ABS and the H(PS-*g*-NR) dispersed phase. This is in accordance with the observation that the ABS/H(PS-*g*-NR) blend at the 10 wt % H(PS-*g*-NR) exhibited the highest tensile strength compared to the other ABS blend samples, and indicates that the H(PS-*g*-NR) acted as the interfacial agent to give a good compatibility with the ABS matrix and improve the mechanical properties of the ABS sheet.

SEM analysis of the fracture surface of ABS/rubber blends at a 20 wt % rubber content, were found to have the lowest tensile strengths compared with the other ABS/rubber ratios, thus revealing the presence of large caves on the fracture surface of the specimens, supporting the observed low mechanical properties of these blends.[28]

CONCLUSIONS

The modification of NR latex was achieved by graft copolymerization as an emulsion using CHPO/TEPA as the redox initiator and then hydrogenated by diimide reaction with N_2H_4 and H_2O_2 and using H_3BO_3 as promoter. Under optimum conditions for the graft copolymerization of ST onto NR (to form PS-*g*-NR), a maximum GE of 81.5% was obtained. The conversion level decreased with decreasing DRC (or increasing water content). For the hydrogenation of PS-*g*-NR, the highest HD (47.2%) was obtained using a 1: 1.1 molar ratio of N_2H_4: H_2O_2 and a H_3BO_3 concentration of 74.7 m*M* at 70°C for 6 h. The H(PS-*g*-NR) particles obtained showed a nonhydrogenated core and a hydrogenated outer layer consistent with a layer model. The decomposition temperature of H(PS-*g*-NR) increased with increasing HD levels, indicating that hydrogenation resulted in an improvement in the thermal stability of the PS-*g*-NR.

The addition of H(PS-*g*-NR) at 10 wt % to ABS increased the tensile strength, elongation at break, and impact strength of the composite blend, and these mechanical properties were stable to heat aging at 165°C for 25 min. Thus, the addition of H(PS-*g*-NR) resulted in a greater heat resistance of the ABS blends than did the addition of NR or PS-*g*-NR. SEM analysis revealed a homogeneous fracture surface of the ABS/H(PS-*g*-NR) blend at 10 wt % H(PS-*g*-NR), supporting the observation of it having the highest tensile strength and also indicating that H(PS-*g*-NR) acted as the interfacial agent to impart the compatibility with ABS and thus improve the mechanical properties of the ABS sheet. In accordance with this finding, TGA revealed the greater thermal stability of the ABS/H(PS-*g*-NR) blend at 10 wt % H(PS-*g*-NR). Therefore, the ABS/hydrogenated grafted NR blend (named "Green ABS") has high potential as a new thermoplastic product for the plastics industry.

ACKNOWLEDGMENTS

Support from the Thai Government Stimulus Package 2 (TKK2555) under the Project for Establishment of Comprehensive Center for Innovative Food, Health Products and Agriculture; the National Research University Project of CHE; and the Ratchadaphiseksomphot Endowment Fund (AM1024I) are gratefully acknowledged.

REFERENCES

1. Oommen, Z.; Thomas, S. *Polym. Bull.* **1993**, *31*, 623.
2. Thiraphattaraphun, L.; Kiatkamjornwong, S.; Prasassarakich, P.; Damronglerd, S. *J. Appl. Polym. Sci.* **2001**, *81*, 428.
3. Arayapranee, W.; Prasassarakich, P.; Rempel, G. L. *J. Appl. Polym. Sci.* **2004**, *93*, 1666.
4. Singha, N. K.; De, P. P.; Sivaram, S. *J. Appl. Polym. Sci.* **1997**, *66*, 1647.
5. Tangthongkul, R.; Prasassarakich, P.; Rempel, G.L. *J. Appl. Polym. Sci.* **2005**, *91*, 2399.
6. Hinchiranan, N.; Prasassarakich, P.; Rempel, G.L. *J. Appl. Polym. Sci.* **2006**, *100*, 4499.
7. Hinchiranan, N.; Charmondusit, K.; Prasassarakich, P.; Rempel, G. L. *J. Appl. Polym. Sci.* **2006**, *100*, 4219.

8. Mahittikul, A.; Prasassarakich, P.; Rempel, G.L. *J. Appl. Polym. Sci.* **2006**, *100*, 640.
9. Mahittikul, A.; Prasassarakich, P.; Rempel, G.L. *J. Appl. Polym. Sci.* **2007**, *103*, 2885.
10. Mahittikul, A.; Prasassarakich, P.; Rempel, G.L. *J. Appl. Polym. Sci.* **2007**, *105*, 1188.
11. Simma, K.; Rempel, G.L.; Prasassarakich, P. *Polym. Degrad. Stab.* **2009**, *94*, 1914.
12. Parker, D. K.; Roberts, R. F.; Schiessl, H. W. *Rubber Chem. Technol.* **1992**, *65*, 245.
13. Arayapranee, W.; Prasassakich, P.; Rempel, G. L. *J. Appl. Polym. Sci.* **2002**, *83*, 2993.
14. Arayapranee, W.; Prasassarakich, P.; Rempel, G. L. *J. Appl. Polym. Sci.* **2003**, *89*, 63.
15. Prasassarakich, P.; Sintoorahat, P.; Wongwisetsirikul, N. *J. Chem. Eng. Jap.* **2001**, *34*, 249.
16. Kochthongrasamee, T.; Prasassarakich, P.; Kiatkamjornwong, S. *J. Appl. Polym. Sci.* **2006**, *101*, 2587.
17. Pukkate, N.; Kitai, T.; Yamamoto, Y.; Kawazura, T.; Sakdapipanich, J.; Kawahara, S. *Eur. Polym. J.* **2007**, *43*, 3208.
18. Suksawad, P.; Yamamoto, Y.; Kawahara, S. *Eur. Polym. J.* **2011**, *47*, 330.
19. Suriyachai, P.; Kiatkamjornwong, S.; Prasassarakich, P. *Rubber Chem. Technol.* **2004**, *77*, 914.
20. Kongparakul, S.; Prasassarakich, P.; Rempel, G. L. *Appl. Catal. A: Gen.* **2008**, *344*, 88.
21. Kongparakul, S.; Prasassarakich, P.; Rempel, G. L. *Eur. Polym. J.* **2009**, *45*, 2358.
22. Wideman, L. G. U.S. Pat. 4,452,950 (**1984**).
23. Parker, D. K.; Roberts, R. F.; Schiessl, H. W. *Rubber Chem. Technol.* **1992**, *65*, 245.
24. Lin, X. L.; Pan, Q.; Rempel, G. L. *J. Appl. Polym. Sci.* **2005**, *96*, 1122.
25. Lin, X. L.; Pan, Q.; Rempel, G. L. *Appl. Catal. A: Gen.* **2004**, *276*, 123.
26. Xie, H. Q.; Li, X. D.; Guo, J. S. *J. Appl. Polym. Sci.* **2002**, *83*, 1375.
27. Sarkar, M. D.; De, P. P.; Browmick, A. K. *J. Appl. Polym. Sci.* **1997**, *66*, 1151.
28. Xu, X. F.; Wang, R.; Tan, Z. Y.; Yang, H. D.; Zhang, M. Y.; Zhang, H. X. *Eur. Polym. J.* **2005**, *41*, 1919.
29. Li, Y.; Shimizu, H. *Eur. Polym. J.* **2009**, *45*, 738.